

Crystal structure of lanthanum oxyorthosilicate, La_2SiO_5

Koichiro Fukuda and Tomoyuki Iwata

Department of Environmental and Materials Engineering, Nagoya Institute of Technology,
Nagoya 466-8555, Japan

Eric Champion

Science des Procédés Céramiques et de Traitements de Surface, Université de Limoges,
UMR CNRS 6638, 123 Avenue Albert Thomas, 87060 Limoges Cedex, France

(Received 11 July 2006; accepted 10 October 2006)

The crystal structure of La_2SiO_5 was refined from laboratory X-ray powder diffraction data ($\text{CuK}\alpha_1$) using the Rietveld method. The crystal structure is monoclinic (space group $P2_1/c, Z=4$) with lattice dimensions $a=0.93320(2)$ nm, $b=0.75088(1)$ nm, $c=0.70332(1)$ nm, $\beta=108.679(1)^\circ$, and $V=0.46687(1)$ nm³. The final reliability indices were $R_{\text{wp}}=7.14\%$, $R_{\text{p}}=5.52\%$, and $R_{\text{B}}=3.83\%$. There are two La sites in the structural model, La1 and La2. La1 is ninefold coordinated to oxygen, forming a tricapped trigonal prism with a mean La1-O distance of 0.263 nm. The La_2O_7 coordination polyhedron is a distorted capped octahedron with a mean La2-O distance of 0.251 nm. The La_1O_9 polyhedra share faces and the La_2O_7 polyhedra share edges, forming two sets of sheets that alternate parallel to the (100) plane. These sheets are linked through SiO_4 tetrahedra and non-silicon-bonded oxygen atoms to form a three-dimensional structure. This compound is isomorphous with the low-temperature (X_1) phases of R_2SiO_5 ($\text{R}=\text{Y}$ and Gd). The volumes of RO_9 polyhedra steadily increase with increasing ionic radius of R, from Y^{3+} to Gd^{3+} to La^{3+} , which causes substantial volumetric expansion of the crystals. © 2006 International Centre for Diffraction Data. [DOI: 10.1154/1.2383066]

Key words: lanthanum oxyorthosilicate, crystal structure, powder diffraction, Rietveld refinement

I. INTRODUCTION

Rare earth (R) oxyorthosilicate of the type R_2SiO_5 have two polymorphs, both of which are monoclinic, with space group $P2_1/c$ for the low-temperature (termed X_1) phase and $I2/a$ for the high-temperature (X_2) phase (Felsche, 1973; Wang *et al.*, 2001; Smolin and Tkachev, 1969; Leonyuk *et al.*, 1999; Maksimov *et al.*, 1970; 1968). The crystal structure of the X_2 phase consists of RO_6 octahedra and SiO_4 tetrahedra. For the X_1 phase, there are two types of R sites; one is coordinated by nine oxygen atoms, while the other is coordinated by seven oxygen atoms. The atomic arrangements in the two structures are quite different from each other; hence, a phase transition from one to the other would be of the reconstructive type. The X_1 phase has been obtained at ambient temperature with the large-radius rare earths: $\text{R}=\text{Yb}$ to La , Y , and Gd (Felsche, 1973; Wang *et al.*, 2001). Structural parameters have been refined for the two compounds Y_2SiO_5 (Wang *et al.*, 2001) and Gd_2SiO_5 (Smolin and Tkachev, 1969). The X_2 phase is metastably obtained at ambient temperature with the smaller rare earths of $\text{R}=\text{Lu}$ to Tb and Y (Felsche, 1973; Maksimov *et al.*, 1970). With an increase of the R ionic radius, the unit-cell volumes of both phases steadily increase. A close relationship has been demonstrated between the lattice deformations induced by thermal expansion and those by cationic substitutions (Fukuda and Matsubara, 2003).

In the present study, we prepared the X_1 phase with the largest ionic radius rare earth, La (La_2SiO_5), to refine the crystal structure from powder diffraction data using the Rietveld method. The volumetric expansion induced by cationic substitutions is discussed in relation to the difference in expansion behavior between the coordination polyhedra RO_9 and RO_7 .

II. EXPERIMENTAL

A specimen of La_2SiO_5 was prepared from stoichiometric amounts of reagent-grade chemicals La_2O_3 and SiO_2 . Well-mixed chemicals were pressed into pellets (12 mm diameter and 3 mm thick), heated at 1773 K for 24 h, followed by quenching in air. Experimental X-ray powder diffraction intensities were collected at 298 K on a PANalytical X'Pert PRO Alpha-1 diffractometer equipped with a high-speed detector (X'Celerator) in the Bragg-Brentano geometry using monochromatized $\text{CuK}\alpha_1$ radiation (45 kV, 40 mA). Other experimental conditions were continuous scan, 2θ range from 14.0042° to 148.4965° , total of 16 097 datapoints, and total experimental time of 21.46 h. The divergence slit of 0.25° was employed to collect the quantitative profile intensities over the whole 2θ range. The crystal-structure models were visualized with the software package VENUS (Izumi and Dilanian, 2002).

III. RESULTS AND DISCUSSION

A. Indexing and structure refinement

Peak positions of the experimental diffraction pattern were first determined using the computer program PowderX (Dong, 1999). The 2θ values of 40 observed peak positions were then used as input data to the automatic indexing program TREOR90 (Werner *et al.*, 1985). One monoclinic cell was found with satisfactory figures of merit $M_{20}/F_{20}=76/104(0.004483, 43)$, $M_{30}/F_{30}=56/88(0.004173, 104)$, and $M_{40}/F_{40}=39/75(0.004402, 122)$ (de Wolff, 1968; Smith and Snyder, 1979). The derived unit-cell parameters of a

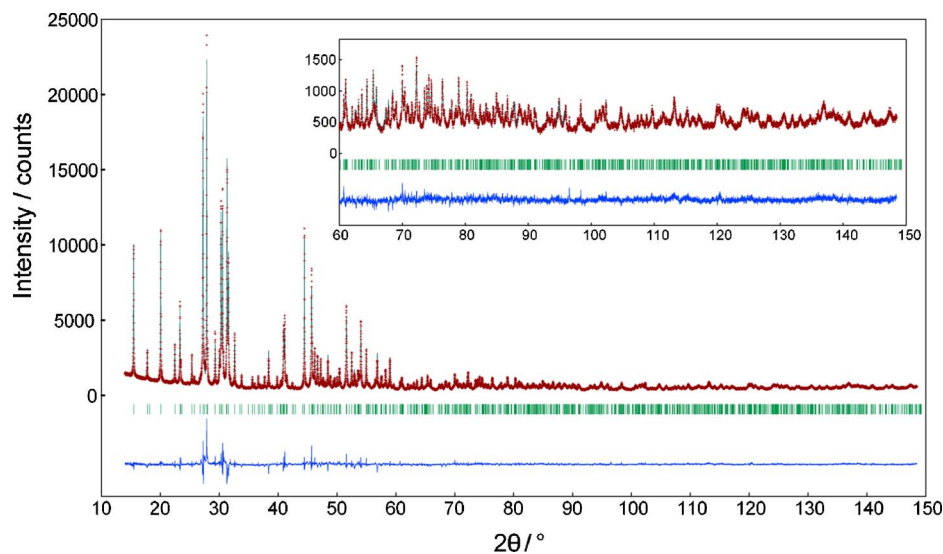


Figure 1. Comparison of the experimental diffraction pattern of lanthanum oxyorthosilicate (symbol: +) with the corresponding calculated pattern (upper solid line). The difference curve is shown in the lower part of the diagram. Vertical bars indicate the positions of possible Bragg reflections.

$=0.93329(5)$ nm, $b=0.75087(3)$ nm, $c=0.70337(4)$ nm, and $\beta=108.675(6)^\circ$ could index all the observed reflections in the experimental diffraction pattern.

The integrated intensities were refined by the whole powder-pattern decomposition method, based on the Pawley algorithm (Pawley, 1981), using program WPPF (Toraya, 1986) from the diffraction data up to $60^\circ 2\theta$. The observed diffraction peaks were examined to determine the presence or absence of reflections. Systematic absences $l \neq 2n$ for $h0l$ and $k \neq 2n$ for $0k0$ reflections were found, which implied that a possible space group was $P2_1/c$. The derived unit-cell parameters and the possible space group were in accord with those of the X_1 phases of R_2SiO_5 ($R=Gd$ and Y). Structural parameters were refined by the Rietveld method using the program RIETAN-2000 (Izumi and Ikeda, 2000) and the experimental powder diffraction data shown in Figure 1. A Legendre polynomial was fitted to background intensities with 12 adjustable parameters. The pseudo-Voigt function (Toraya, 1990) was used to fit the experimental peak profiles. All of the isotropic atomic displacement parameters (B) of oxygen atoms were constrained to have the same value. The final reliability indices were $R_{wp}=7.14\%$ ($S=2.01$), $R_p=5.52\%$, and $R_B=3.83\%$ (Young, 1993). Crystal data are given in Table I, and the final positional and B parameters of atoms are given in Table II.

TABLE I. Crystal data for La_2SiO_5 .

	La_2SiO_5
Chemical composition	La_2SiO_5
Space group	$P2_1/c$
a/nm	0.93320(2)
b/nm	0.75088(1)
c/nm	0.70332(1)
$\beta/^\circ$	108.679(1)
V/nm^3	0.46687(1)
Z	4
D_x/Mgm^{-3}	5.49

B. Structure description and discussion

Figure 2 shows sections of the crystal structure of La_2SiO_5 . Selected interatomic distances and bond angles, together with their standard deviations, are listed in Table III. The mean Si–O bond length of 0.163 nm in the SiO_4 tetrahedra is in good agreement with that expected from the bond valence sum (0.162 nm). The mean value of the O–Si–O angles is 109° . These values are in good agreement with those found in other silicates (Baur, 1971).

There are two La sites in the structural model, La1 and La2. The La1 atom is coordinated to nine oxygen atoms, forming a tricapped trigonal prism with bond lengths ranging from 0.237 to 0.305 nm (mean=0.263 nm). A similar geometry around the La atom has been described in sodium lanthanum diphosphate $NaLaP_2O_4$ (mean=0.260 nm) (Ferid and Horchani-Naifer, 2004). The La2 atom is sevenfold coordinated with a mean La2–O distance of 0.251 nm, which is comparable to those of the two types of LaO_7 polyhedra in lanthanum aurate, $La_4Au_2O_9$ (mean=0.250 nm) (Ralle and Jansen, 1994). The ratio of the volume of the circumscribed sphere to that of the polyhedron (V_S/V_P) for La_2O_7 is 2.94. Because the V_S/V_P values of the ideal pentagonal bipyramid and the ideal capped octahedron are 2.643 and 3.049, respectively (Makovicky and Balic-Zunic, 1998), the present La_2O_7 polyhedron can be described as a distorted capped

TABLE II. Atomic and thermal parameters for La_2SiO_5 .

Atom	Site	x	y	z	$100 \times B$ (nm^2)
La1	4e	0.1117(1)	0.1541(1)	0.4055(1)	0.79(2)
La2	4e	0.5116(1)	0.6238(1)	0.2352(1)	0.75(2)
Si	4e	0.2008(4)	0.5775(5)	0.4579(6)	0.19(9)
O1	4e	0.191(1)	0.4422(8)	0.634(1)	0.23(8)
O2	4e	0.1372(9)	0.4703(9)	0.247(1)	0.23
O3	4e	0.3771(8)	0.636(1)	0.503(1)	0.23
O4	4e	0.0942(9)	0.7502(9)	0.445(1)	0.23
O5	4e	0.3932(8)	0.373(1)	0.060(1)	0.23

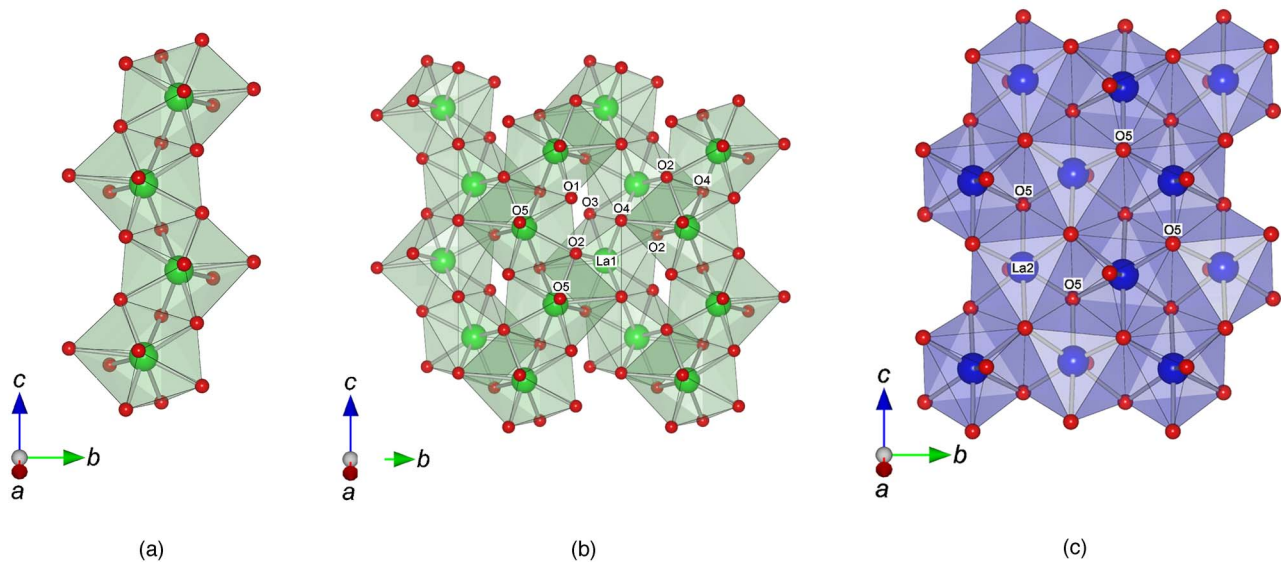


Figure 2. Projection of part of the structure viewed along the a^* axis. Atom numbering corresponds to that given in Table II. (a) The La_1O_9 polyhedra share faces to form a chain running parallel to $\langle 001 \rangle$. (b) The La_1O_9 polyhedral chains are linked via O4-O2-O4-O2 faces. (c) Edge-sharing La_2O_7 polyhedra form a sheet parallel to (100) at $x \sim 0.5$.

octahedron. The bond valence sums calculated on the basis of bond-strength analysis (La1:2.86, La2:3.00, Si:3.98) are in good agreement with expected formal oxidation states of La^{3+} and Si^{4+} ions (Brown and Altermatt, 1985; Brese and O'Keeffe, 1991).

The ionic radius of La^{3+} in ninefold coordination [$r(\text{La}^{3+}(9))=0.1216$ nm and $r(\text{O}^{2-}(8))=0.142$ nm] and that of La^{3+} in sevenfold coordination [$r(\text{La}^{3+}(7))=0.110$ nm and $r(\text{O}^{2-}(6))=0.140$ nm] predict interatomic distances of 0.264 and 0.250 nm for La1-O and La2-O, respectively (Shannon, 1976). These predicted values are in good agreement with the corresponding mean interatomic distances ($\langle \text{La1-O} \rangle = 0.263$ nm and $\langle \text{La2-O} \rangle = 0.251$ nm). The mean interatomic

distances are also in agreement with those expected from the bond valence sum (0.258 nm for La1-O and 0.249 nm for La2-O).

The crystal structure of La_2SiO_5 consists of the three types of polyhedra: La_1O_9 , La_2O_7 , and SiO_4 . The La_1O_9 polyhedra share faces to form infinite chains running parallel to $\langle 001 \rangle$ [Figure 2(a)]. Individual chains are further linked via O4-O2-O4-O2 faces of the La_1O_9 polyhedra [Figure 2(b)]. The La_2O_7 polyhedra share edges, resulting in a formation of sheets parallel also to the (100) plane at $x \sim 0.5$ [Figure 2(c)]. These two types of polyhedral groups are alternately stacked parallel to (100), and they are intercon-

TABLE III. Selected interatomic distances (nm) and angles ($^\circ$).

La1-O1	0.2654(7)	La2-O1 ^f	0.2676(9)	Si-O1	0.163(1)
La1-O1 ^a	0.237(1)	La2-O3	0.2575(9)	Si-O2	0.1624(9)
La1-O2	0.2666(8)	La2-O3 ^f	0.2656(8)	Si-O3	0.1634(9)
La1-O2 ^b	0.2618(8)	La2-O3 ^g	0.2489(8)	Si-O4	0.1619(9)
La1-O2 ^c	0.2516(9)	La2-O5	0.2324(8)	O1-Si-O2	107.0(5)
La1-O4 ^d	0.3055(7)	La2-O5 ^h	0.2506(9)	O1-Si-O3	108.7(5)
La1-O4 ^e	0.257(1)	La2-O5 ⁱ	0.2358(8)	O1-Si-O4	111.0(5)
La1-O4 ^b	0.2695(7)			O2-Si-O3	111.0(5)
La1-O5 ^c	0.2509(8)			O2-Si-O4	108.0(5)
				O3-Si-O4	111.0(5)

Symmetry transformations used to generate equivalent atoms:

^a $x, 1/2-y, -1/2+z.$

^b $-x, -1/2+y, 1/2-z.$

^c $x, 1/2-y, 1/2+z.$

^d $x, -1+y, z.$

^e $-x, 1-y, 1-z.$

^f $1-x, 1-y, 1-z.$

^g $x, 3/2-y, -1/2+z.$

^h $1-x, 1-y, -z.$

ⁱ $1-x, 1/2+y, 1/2-z.$

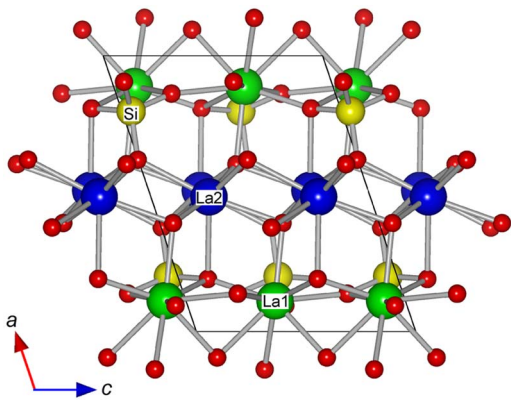


Figure 3. Crystal structure of lanthanum oxyorthosilicate viewed along the b axis.

nected via SiO_4 groups and non-silicon-bonded oxygen atoms (O5) to form a three-dimensional structure (Figure 3).

La_2SiO_5 has been found to be isostructural with the X_1 -phases of Y_2SiO_5 and Gd_2SiO_5 . The volumes of RO_9 polyhedra ($R = \text{Y, Gd, and La}$) steadily increase with increasing ionic radius of R (r_R) (Figure 4). The polyhedral volume for LaO_9 is about 1.3 times larger than that of YO_9 . For the RO_7 polyhedra, the volumes also tend to increase with increasing r_R , however the increases are much smaller than those of RO_9 . The unit-cell volumes also increase steadily with increasing r_R (Felsche, 1973; Wang *et al.*, 2001), and the cell volume of La_2SiO_5 ($=0.4669 \text{ nm}^3$) is about 1.2 times as large as that of Y_2SiO_5 ($=0.3974 \text{ nm}^3$). Accordingly, the increase in the cell volume that is induced by the cationic substitution is mainly attributable to the volumetric expansion of the RO_9 polyhedra.

IV. CONCLUSION

We refined the crystal structure of La_2SiO_5 , which has a monoclinic unit cell with space group $P2_1/c$. This compound

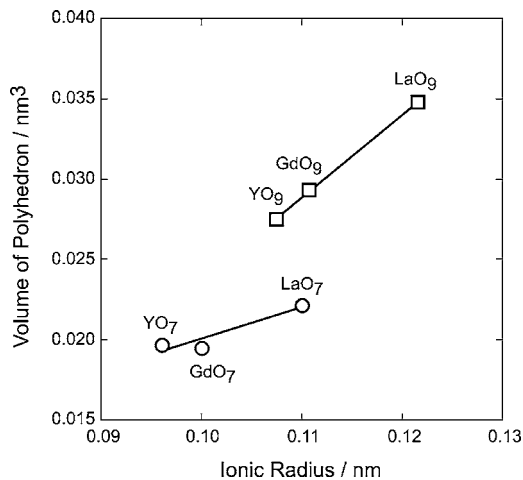


Figure 4. Changes in polyhedral volumes with effective ionic radius of the rare earths.

is isomorphous with the X_1 -phases of R_2SiO_5 ($R = \text{Y and Gd}$). The crystal structure consists of three types of polyhedra: LaO_9 , LaO_7 , and SiO_4 . The unit-cell volumes increase steadily with increasing ionic radius of R , from Y^{3+} to Gd^{3+} to La^{3+} . The increase in the unit-cell volume is mainly attributable to the volumetric expansion of the RO_9 polyhedra.

- Baur, W. H. (1971). "Prediction of bond length variations in silicon-oxygen bonds," *Am. Mineral.* **56**, 1573–1599.
- Breese, N. E. and O'Keeffe, M. (1991). "Bond-valence parameters for solids," *Acta Crystallogr.* **47**, 192–197.
- Brown, I. D. and Altermatt, D. (1985). "Bond-valence parameters obtained from a systematic analysis of the inorganic crystal structure database," *Acta Crystallogr.* **41**, 244–247.
- Dong, C. (1999). "Windows-95-based program for powder X-ray diffraction data processing," *J. Appl. Crystallogr.* **32**, 838.
- Felsche, J. (1973). "The crystal chemistry of the rare-earth silicates" in *Structure and Bonding*, edited by J. D. Dunitz, P. Hemmerich, J. A. Ibers, C. K. Jorgensen, J. B. Neilands, Sir R. S. Nyholm, D. Reinen, R. J. P. Williams (Springer-Verlag, Berlin), Vol. 13, pp. 99–197.
- Ferid, M. and Horchani-Naifer, K. (2004). "Synthesis, crystal structure and vibrational spectra of a new form of diphosphate NaLaP_2O_7 ," *Mater. Res. Bull.* **39**, 2209–2217.
- Fukuda, K. and Matsubara, H. (2003). "Anisotropic thermal expansion in yttrium silicate," *J. Mater. Res.* **18**, 1715–1722.
- Izumi, F. and Dilanian, R. A. (2002). "Structure refinement based on the maximum-entropy method from powder diffraction data" in *Recent Research Developments in Physics*, (Transworld Research Network, Trivandrum, India), Vol. 3, Part II, pp. 699–726.
- Izumi, F., and Ikeda, T. (2000). "A Rietveld-analysis program RIETAN-98 and its applications to zeolites," *Mater. Sci. Forum* **321–324**, 198–203.
- Leonyuk, N. I., Belokoneva, E. L., Bocelli, G., Right, L., Shvanskii, E. V., Henrykhon, R. V., Kulman, N. V., and Kozhbakhteeva, D. E. (1999). "Crystal growth and structural refinements of the Y_2SiO_5 , Y_2SiO_7 and LaBSiO_5 single crystals," *Cryst. Res. Technol.* **34**, 1175–1182.
- Makovicky, E., and Balic-Zunic, T. (1998). "New measure of distortion for coordination polyhedra," *Acta Crystallogr.* **54**, 766–773.
- Maksimov, B. A., Kharitonov, Y. A., Ilyukhin, V. V., and Belov, N. V. (1968). "Crystal structure of yttrium oxyorthosilicate," *Dokl. Akad. Nauk SSSR* **183**, 1072–1075.
- Maksimov, B. A., Ilyukhin, V. V., Kharitonov, Y. A., and Belov, N. V. (1970). "Crystal structure of yttrium oxyorthosilicate $\text{Y}_2\text{O}_3 \cdot \text{SiO}_2 = \text{Y}_2\text{SiO}_5$," *Kristallografiya* **15**, 926–933.
- Pawley, G. S. (1981). "Unit-cell refinement from powder diffraction scans," *J. Appl. Crystallogr.* **14**, 357–361.
- Ralle, M. and Jansen, M. (1994). "Preparation and crystal structure of new lanthanum aurates $\text{La}_4\text{Au}_2\text{O}_9$," *J. Alloys Compd.* **203**, 7–13.
- Shannon, R. D. (1976). "Revised effective ionic radii and systematic studies of interatomic distances in halides and chalcogenides," *Acta Crystallogr.* **32**, 751–767.
- Smith, G. S. and Snyder, R. L. (1979). " F_N : A criterion for rating powder diffraction patterns and evaluating the reliability of powder-pattern indexing," *J. Appl. Crystallogr.* **12**, 60–65.
- Smolin, Y. I. and Tkachev, S. P. (1969). "Determination of the structure of gadolinium orthosilicate $\text{Gd}_2\text{O}_3 \cdot \text{SiO}_2$," *Kristallografiya* **14**, 22–25.
- Toraya, H. (1986). "Whole-powder-pattern fitting without reference to a structural model: application to X-ray powder diffractometer data," *J. Appl. Crystallogr.* **19**, 440–447.
- Toraya, H. (1990). "Array-type universal profile function for powder pattern fitting," *J. Appl. Crystallogr.* **23**, 485–491.
- Wang, J., Tian, S., Li, G., Liao, F., and Jing, X. (2001). "Preparation and X-ray characterization of low-temperature phases of R_2SiO_5 ($R = \text{Rare Earth Elements}$)," *Mater. Res. Bull.* **36**, 1855–1861.
- Werner, P.-E., Eriksson, L., and Westdahl, M. (1985). "TREOR, a semi-exhaustive trial-and-error powder indexing program for all symmetries," *J. Appl. Crystallogr.* **18**, 367–370.
- de Wolff, P. M. (1968). "A simplified criterion for the reliability of a powder pattern indexing," *J. Appl. Crystallogr.* **1**, 108–113.
- Young, R. A. (1993). "Introduction to the Rietveld method," in *The Rietveld Method*, edited by R. A. Young (Oxford U.P., Oxford), pp. 1–38.